Biophysical Journal
Article

Biophysical Society

Reconstitution of Human Ion Channels into Solvent-free Lipid Bilayers Enhanced by Centrifugal Forces

Ayumi Hirano-Iwata,[1,*] Yutaka Ishinari,[1] Miyu Yoshida,[1] Shun Araki,[1] Daisuke Tadaki,[1] Ryusuke Miyata,[1] Kenichi Ishibashi,[2] Hideaki Yamamoto,[3] Yasuo Kimura,[4] and Michio Niwano[1,5]

[1]Graduate School of Biomedical Engineering, Tohoku University, Aoba, Sendai, Japan; [2]Hang-Ichi Corporation, Naka, Yokohama, Japan; [3]Frontier Research Institute for Interdisciplinary Sciences, Tohoku University, Aoba, Sendai, Japan; [4]Department of Electric and Electronic Engineering, School of Engineering, Tokyo University of Technology, Hachioji, Tokyo, Japan; and [5]Laboratory for Nanoelectronics and Spintronics, Research Institute of Electrical Communication, Tohoku University, Aoba, Sendai, Japan

ABSTRACT Artificially formed bilayer lipid membranes (BLMs) provide well-defined systems for functional analyses of various membrane proteins, including ion channels. However, difficulties associated with the integration of membrane proteins into BLMs limit the experimental efficiency and usefulness of such BLM reconstitution systems. Here, we report on the use of centrifugation to more efficiently reconstitute human ion channels in solvent-free BLMs. The method improves the probability of membrane fusion. Membrane vesicles containing the human *ether-a-go-go*-related gene (hERG) channel, the human cardiac sodium channel ($Na_v1.5$), and the human $GABA_A$ receptor ($GABA_AR$) channel were formed, and the functional reconstitution of the channels into BLMs via vesicle fusion was investigated. Ion channel currents were recorded in 67% of the BLMs that were centrifuged with membrane vesicles under appropriate centrifugal conditions (14–55 $\times$ *g*). The characteristic channel properties were retained for hERG, $Na_v1.5$, and $GABA_AR$ channels after centrifugal incorporation into the BLMs. A comparison of the centrifugal force with reported values for the fusion force revealed that a centrifugal enhancement in vesicle fusion was attained, not by accelerating the fusion process but by accelerating the delivery of membrane vesicles to the surface of the BLMs, which led to an increase in the number of membrane vesicles that were available for fusion. Our method for enhancing the probability of vesicle fusion promises to dramatically increase the experimental efficiency of BLM reconstitution systems, leading to the realization of a BLM-based, high-throughput platform for functional assays of various membrane proteins.

INTRODUCTION

The lipid bilayer, a basic constituent of the cell membrane, is a major barrier against ion movement, and specific membrane proteins permit ions to pass through it. Among these, ion channels provide gated pores that allow ion permeation following electrochemical gradients. Owing to their crucial roles in regulating transmembrane signaling, ion channel proteins are major targets for drug design (1,2). There is a growing interest in the development of drug-screening platforms for ion channels because a wide range of ion channels have been identified not only as primary molecular targets in drug actions but also as major targets in drug-induced side effects (3,4). Recording ion-channel activities by measuring ion currents is an efficient method for investigating the functions of channels and screening for both beneficial and adverse effects of drug candidates (3). Although the patch-clamp method is considered to be the gold standard for evaluating channel activities, the method also has limitations in that the observed currents are dependent on the condition of the target cells (3). Therefore, the development of an alternate method for recording ion channel activities, complementing the patch-clamp method, would be highly desirable (5).

Reconstitution of ion channel proteins in artificial free-standing bilayer lipid membranes (BLMs) is another approach for recording ion channel activities (5,6). The BLM reconstitution system has the advantage that the researcher can control the composition of the system, including the solution phase and the lipid environment. However, two major problems associated with BLM systems reduce experimental efficiency and prevent them from being widely used, namely, membrane instability and a low efficiency of ion channel incorporation into BLMs.

The simplest way to improve the stability of BLMs is to decrease the size of freestanding BLMs using nanofabricated apertures (7–10); however, a reduced BLM area makes it more difficult to incorporate ion channel proteins, especially channels of pharmaceutical interest. To overcome

Submitted November 30, 2015, and accepted for publication April 11, 2016.

*Correspondence: ahirano@bme.tohoku.ac.jp

Editor: Simon Scheuring.

http://dx.doi.org/10.1016/j.bpj.2016.04.010

this trade-off, we proposed a new, to our knowledge, concept for BLM stabilization (11). We fabricated relatively large apertures (several tens of micrometers in diameter), the edges of which were smoothly tapered to the nanoscale. BLMs that formed in the tapered aperture showed a tolerance to mechanical shock during repetitive solution exchanges, and had a lifetime in excess of 60 h when human *ether-a-go-go* related gene (hERG) channels were incorporated (12). The tapered aperture edge reduces stress on the bilayer at the point of contact with the edge, leading to increased BLM stability. A similar enhancement in BLM stability based on tapered apertures was also reported by Eray et al. (13) and Kalsi et al. (14). The key feature of this approach is that one can form mechanically stable BLMs while maintaining a large membrane area of several tens of micrometers.

One of the most critical steps in the formation of channel-embedded stable BLMs is the integration of ion channels into BLMs (5,15,16). Ion channel proteins of pharmaceutical interest are generally extracted from tissues or cell lines that overexpress the channels and are then reconstituted into lipid vesicles to form proteoliposomes or membrane vesicles. To incorporate the channels into BLMs, it is necessary to fuse the proteoliposomes (membrane vesicles) with BLMs (vesicle fusion) (Fig. 1 *a*). Since vesicle fusion between vesicles and BLMs is also regarded as a model system for biological exocytosis, a ubiquitous secretion event in eukaryotic cells (17), factors that affect the efficiency of vesicle fusion have been intensively studied. For example, an osmotic salt gradient across BLMs (18,19) and the presence of nystatin-ergosterol complexes in proteoliposomes (20–22) are often effective in promoting vesicle fusion. In another approach, vesicles are first fused to a lipid monolayer at the air/water or air/oil interface and the channel-containing lipid monolayer is then hybridized with another lipid monolayer (23–25). These approaches have been utilized to incorporate eukaryotic channels into BLMs formed in various microfabricated devices (12,23–27). However, most of the BLMs contained nonvolatile organic solvents, such as *n*-decane and *n*-hexadecane, which probably are not present in naturally occurring cell membranes.

The use of a nonvolatile hydrocarbon solvent is a common approach not only to improve BLM stability but also to promote channel integration (7–14,18–22,24–29). Several researchers reported that the presence of nonvolatile organic solvent in BLMs appeared to promote channel reconstitution (28,29). It was proposed that interactions between vesicles and BLMs occur predominantly in regions where a hydrocarbon solvent is present (28,30). The presence of exogenous solvents in BLMs, however, may alter the behavior and function of ion channels that are embedded within them. Therefore, it would be desirable to develop an efficient method for incorporating ion channels into solvent-free BLMs, which would have fewer potential fusion sites compared with solvent-containing BLMs.

In this study, we report on the centrifugal acceleration of vesicle fusion with solvent-free and mechanically stable BLMs. Our approach for increasing the efficiency of fusion involved increasing the number of membrane vesicles delivered to the surface of BLMs by using centrifugal force. The stable BLMs, when formed in the tapered apertures in microfabricated silicon (Si) chips, tolerated the applied centrifugal force. Functional reconstitution of human channels, such as the hERG channel, the human cardiac sodium ($Na_v1.5$) channel, and the human $GABA_A$ receptor ($GABA_AR$) channel, was examined through vesicle fusion under centrifugation. Ion currents of single or multiple channels and the efficiency of channel incorporation were investigated.

MATERIALS AND METHODS

Cell lines and reagents

Chinese hamster ovary (CHO) cell lines expressing the hERG channels (Kv11.1) were obtained from the Channelopathy Foundation (Basel, Switzerland). Human embryonic kidney (HEK) 293 cell lines expressing the human $Na_v1.5$ and human $\alpha1\beta2\gamma2$ $GABA_AR$ channels were obtained from Anaxon AG (Berne, Switzerland). These cell lines were cultured in

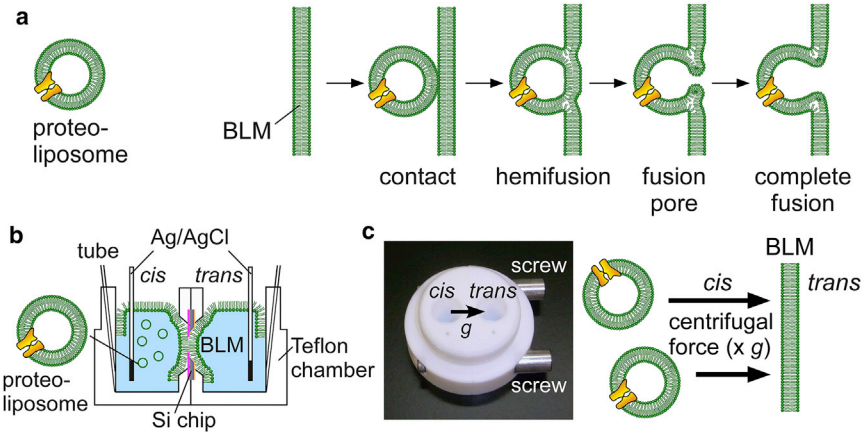

FIGURE 1 (*a*) Schematic diagram of the sequence of steps for fusing a vesicle with a BLM. (*b*) Schematic of membrane vesicles and a BLM formed across a microaperture in an Si chip (not drawn to scale). (*c*) Photograph of the Teflon chamber used for channel incorporation using centrifugation (*left*), and a strategy for enhancing reconstitution by using centrifugal force to deliver membrane vesicles to the BLM surface (*right*). Centrifugal force was applied in the direction from the *cis* side to the *trans* side. To see this figure in color, go online.

a 37°C incubator with 5% CO_2 according to the manufacturer's protocol. CHO cell lines expressing hERG channels were maintained in HAM/F-12 medium supplemented with 10% fetal bovine serum (FBS), 1% penicillin/streptomycin, and 100 μg/mL hygromycin B (GIBCO). HEK 293 cell lines expressing $Na_v1.5$ and $GABA_AR$ channels were maintained in Dulbecco's modified Eagle's medium/GlutaMAX medium supplemented with 10% FBS, 1% penicillin/streptomycin under an antibiotic pressure of 100 μg/mL zeocin (GIBCO) and 100 μg/mL geneticin (GIBCO), respectively. Chloroform solutions of L-α-phosphatidylcholine (from egg) and L-α-phosphatidylethanolamine (transphosphatidylated (egg)) were purchased from Avanti Polar Lipids (Alabaster, AL). Cholesterol was obtained from Wako Pure Chemicals (Osaka, Japan) and recrystallized three times from methanol. Tetrodotoxin (TTX) was purchased from Wako Pure Chemicals. Picrotoxin was obtained from Sigma-Aldrich (St. Louis, MO).

Protein isolation

The hERG channels were extracted from CHO cell lines as membrane fractions according to the procedures described by Oshima et al. (12). The $GABA_AR$ channels were isolated from HEK 293 cell lines in the same manner, except that the final membrane pellets were resuspended in 140 mM NaCl, 5 mM KCl, 2 mM $CaCl_2$, 1 mM $MgCl_2$, 10 mM D-glucose, 10 mM HEPES (pH 7.4 with NaOH). The $Na_v1.5$ channels were also isolated from HEK 293 cell lines in the same manner, except that the cells from 100-mm plates were scraped off into a 3-mL solution of 200 mM KCl, 33 mM KF, 10 mM EDTA, 50 mM HEPES (pH 7.4 with KOH) plus protease inhibitors (100 μM phenylmethylsulfonyl fluoride, 1 μg/mL pepstatin A, 1 μg/mL leupeptin), and the final membrane pellets were resuspended in 149.2 mM NaCl, 4.7 mM KCl, 2.5 mM $CaCl_2$, 5.0 mM HEPES (pH 7.3 with NaOH).

BLM formation and protein incorporation via centrifugation

Microapertures (Φ: 18–55 μm) with tapered edges were fabricated in Si chips, and the surface of the chip was coated with a thermal oxide and Teflon-AF (DuPont Fluoroproducts, Wilmington, DE) (Fig. S1 in the Supporting Material) according to the procedure described by Oshima et al. (31). Details of chip fabrication are given in Supporting Materials and Methods. The Si chip was silanized by treating it with 2% (v/v) 3-cyanopropyldimethylchlorosilane (Gelest, Morrisville, PA) in acetonitrile for 1–2 h at room temperature in a nitrogen-filled glove box. Planar BLMs were formed across the microaperture by folding up two lipid monolayers (Fig. 1 *b*) according to Oshima et al. (12), except that the *n*-hexadecane coating around the aperture was omitted to form solvent-free BLMs. The BLMs were formed in symmetric recording solutions: 120 mM KCl, 10 mM HEPES (pH 7.2 with KOH) for hERG channels; 149.2 mM NaCl, 4.7 mM KCl, 2.5 mM $CaCl_2$, 5.0 mM HEPES (pH 7.3 with NaOH) for $Na_v1.5$ channels; and 140 mM NaCl, 5 mM KCl, 2 mM $CaCl_2$, 1 mM $MgCl_2$, 10 mM D-glucose, 10 mM HEPES (pH 7.4 with NaOH) for $GABA_AR$ channels. Solvent-free BLMs with resistances of $>$10 GΩ and $>$100 GΩ were formed in the Si chips with success probabilities of 85% and 75%, respectively, from 134 trials.

A suspension (typically 100 μL) of membrane vesicles containing channel proteins was added to the *cis* solution after formation of the BLMs. The water level of *cis* and *trans* compartments in a Teflon chamber was adjusted to the top surface of the chamber by adding recording solutions (a total of 1700 μL for both compartments). The Teflon chamber was sealed with a lid and then spun using a Kubota centrifuge (model 3740) (Fig. 1 *c*). For the purpose of comparison, incorporation of hERG channels by stirring was also examined according to the procedures described by Oshima et al. (12).

Current recordings

Current recordings were performed with an Axopatch 200B patch-clamp amplifier (Molecular Devices, Sunnyvale, CA). Signals were filtered online at 1–2 kHz with a low-pass Bessel filter, digitized at 10–20 kHz, and stored online using a data acquisition system (Digidata 1440 and pCLAMP 10.2; Molecular Devices). In the case of hERG channels, the currents were filtered offline at a cutoff frequency of 0.7 kHz according to a literature report (32). Applied potentials were defined with respect to the *trans* side held at ground.

Atomic force microscopy

An Si chip without an aperture was silanized with 3-cyanopropyldimethylchlorosilane and centrifuged with a suspension of membrane vesicles containing hERG channels in the same manner as Si chips suspending BLMs (Fig. 2 *a*). After the solutions in both compartments were discarded, the Si chip was removed from the chamber and air dried. Tapping-mode atomic force microscopy (AFM) images of the Si chip surface were obtained by using Dimension Icon NanoScopeV (Veeco Instruments, Plainview, NY). The AFM observation was performed in air.

RESULTS AND DISCUSSION

Use of centrifugal force to accelerate vesicle fusion to incorporate ion channels into BLMs

Vesicle fusion between proteoliposomes (or membrane vesicles) and lipid bilayers is a critical step for channel incorporation into BLM reconstitution systems, as well as a model for exocytosis in biological membranes. Several key intermediate states have been identified for vesicle fusion: contact, hemifusion, formation of a fusion pore, and complete fusion (Fig. 1 *a*) (33,34). Chanturiya et al. (33) carefully counted the number of respective intermediates during fusion between liposome vesicles and freestanding BLMs. They reported that only 16% of the vesicles reached the hemifusion state, suggesting that most of the vesicles were lost before reaching the BLMs. Although due to methodological limitations of their approach, it is still unclear whether the contact or hemifusion state is more critical for attaining complete fusion, the access of vesicles to BLMs might be a key factor in accelerating the vesicle fusion.

We first investigated the issue of whether centrifugal force could be used to improve the accessibility of membrane vesicles to BLMs. Si chips without apertures were centrifuged with a suspension of membrane vesicles containing hERG channels in the same manner as Si chips suspending BLMs (Fig. 2 *a*), and the surface topography of the chips was then analyzed by AFM (Fig. 2, *b–f*). The hERG channel is a voltage-gated potassium channel that is crucial for repolarization during action potentials in the human heart (35,36). This channel has attracted pharmaceutical attention because a diverse group of drugs have been found to adversely block hERG channels, resulting in potentially fatal arrhythmias (35,36). When membrane vesicles were centrifuged at 500 rpm (14 $\times$ *g*) for 10 min, vesicle precipitates were observed on the surface of the Si chips (Fig. 2 *d*).

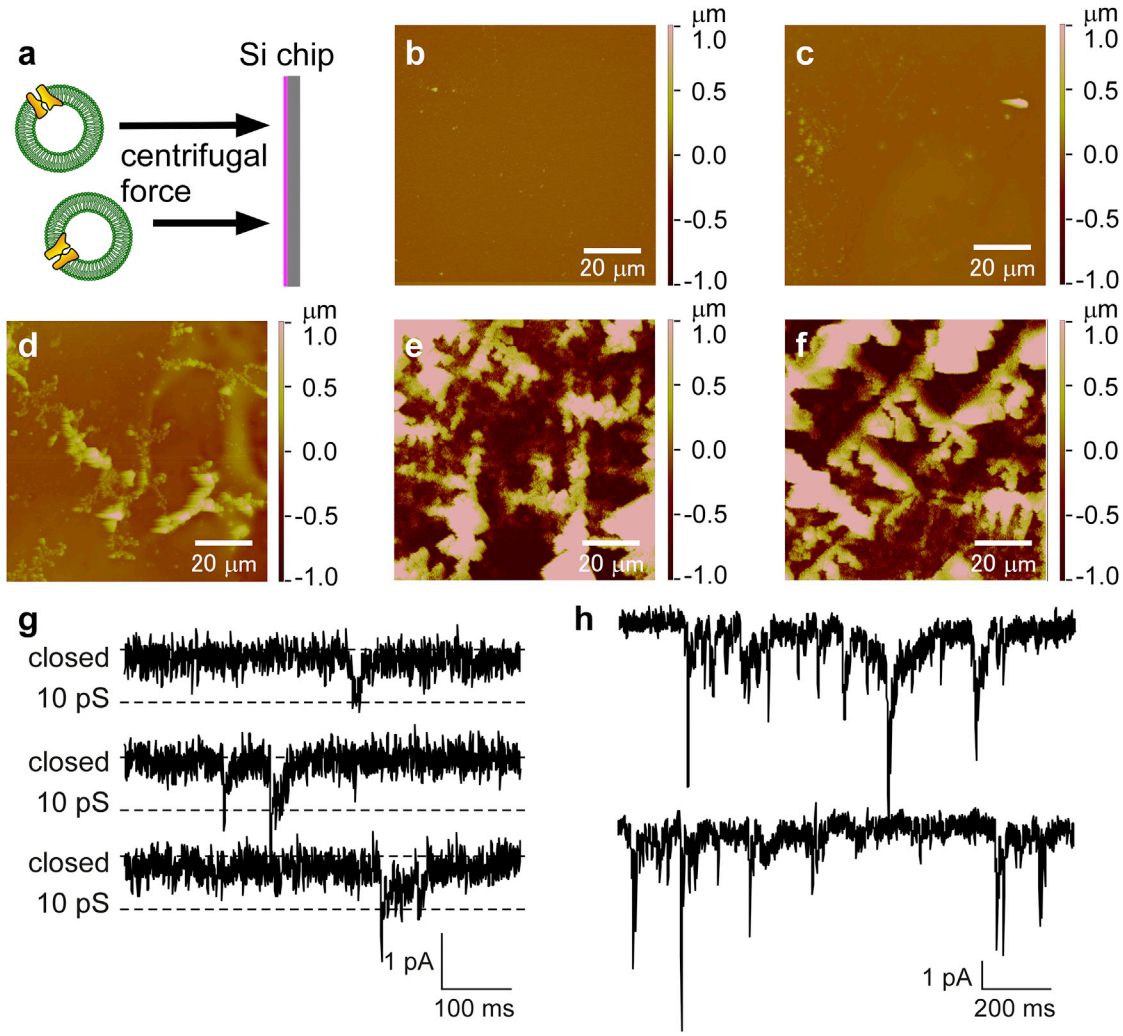

FIGURE 2 Centrifugal force as a driving force to improve the accessibility of membrane vesicles to BLMs. (*a*) Si chips with no apertures were centrifuged in the presence and absence of membrane vesicles containing hERG channels. (*b–f*) The surface topography of the chips after centrifugation was analyzed by AFM. Conditions for centrifugations: (*b*) 1000 rpm for 10 min without membrane vesicles, (*c*) 300 rpm for 30 min with membrane vesicles containing hERG channels, and (*d–f*) 10 min centrifugation with membrane vesicles containing hERG channels at (*d*) 500 rpm, (*e*) 800 rpm, and (*f*) 1000 rpm. The middle area (90 μm × 90 μm) of the Si chip was scanned. This area covers the region of the BLMs (Φ: 18–55 μm) in the case of Si chips suspending BLMs. (*g*) Example of single hERG channel currents recorded after centrifugation at 500 rpm for 10 min. The applied potential was −100 mV. (*h*) Example of multiple hERG channel currents recorded after centrifugation at 500 rpm for 10 min. The applied potential was −100 mV. To see this figure in color, go online.

At higher centrifugal forces of 800 rpm (35 × *g*) and 1000 rpm (55 × *g*), larger amounts of precipitates were observed (Fig. 2, *e* and *f*). Such precipitates were only observed in cases where the Si chips were centrifuged with membrane vesicles. Centrifugation at 1000 rpm without membrane vesicles resulted in a flat topography over the entire area scanned (Fig. 2 *b*). A lower centrifugal force of 300 rpm (4.9 × *g*) was insufficient to deliver membrane vesicles, and the amount of precipitate was negligible, even when the centrifugation was prolonged for 30 min (Fig. 2 *c*). These results indicate that a centrifugal force of ≥500 rpm is sufficient for delivering channel-containing membrane vesicles to the surface of BLMs, leading to an increase in the number of vesicles in contact with the BLMs.

We then examined the effect of centrifugation on the efficiency of fusion between membrane vesicles and BLMs that were formed in the tapered microapertures. The BLMs were centrifuged with membrane vesicles containing hERG channels, and the probability of recording ion-channel currents was investigated. Fig. 2 *g* shows example traces of single-channel currents, which were recorded after centrifugation at 500 rpm for 10 min. The observed single-channel conductance (10 pS) was consistent with previously reported values (11–12 pS in 120 mM KCl) obtained with a BLM reconstitution system (12,37) and the patch-clamp method (32). In some cases, multiple channels were incorporated into BLMs after the centrifugation, showing larger bursting currents (Fig. 2 *h*) whose shape was similar to that of previously reported hERG multichannel currents

(12). The probability of observing either single- or multichannel activities (incorporation probability) was 67% (Fig. 3) under conditions in which vesicle fusion was performed under centrifugation at 500–1000 rpm for 10–20 min. The probability decreased to 20% with centrifugation at 300 rpm for 10–70 min, reflecting a decreased driving force for delivering membrane vesicles to the surface of BLMs. When vesicle fusion was performed by stirring, the incorporation probability was much lower (5.8%), even when the stirring was continued for an extended period of time (several hours). These results indicate the potential of using centrifugal force at $\geq$500 rpm ($\geq 14 \times g$) to accelerate fusion of membrane vesicles with BLMs.

Incorporation of human $Na_v1.5$ and $GABA_AR$ channels into BLMs using centrifugation

To further explore the use of centrifugation to enhance the fusion probability between membrane vesicles and BLMs, we next examined the incorporation of other human channels with different gating mechanisms, i.e., a voltage-gated sodium channel ($Na_v1.5$) and a ligand-gated channel ($GABA_AR$).

$Na_v1.5$ is the major voltage-gated sodium channel in the heart and is essential for the initiation and propagation of cardiac action potentials (38). Since blockade of this channel by a drug can result in blockade of ventricular conductance and potentially serious arrhythmias, this channel is also an important target for drug safety screenings (4). When membrane vesicles containing $Na_v1.5$ channels were centrifuged with the BLMs at 800–900 rpm for 5–10 min, both single- and multichannel currents were frequently observed (Fig. 4). From single-channel traces, stepwise currents were observed with a single-channel conductance of 20 pS. This conductance level is similar to a previously reported value (17 pS in 149.2 mM NaCl) for $Na_v1.5$ channels expressed in HEK 293 cells (39). The single-channel current showed a linear relation to the applied potential, which is in agreement with previously reported patch-clamp observations for $Na_v1.5$ (39,40). All channel activities were observed using the same voltage protocol shown in Fig. 4 *a* with a strong hyperpolarizing prestep, which is a typical protocol for the $Na_v1.5$ channel in patch-clamp studies (39,41). The addition of TTX, a specific blocker for Na channels, to the *trans* side solution completely blocked single- and multichannel activities. These channel properties confirmed the functional incorporation of the $Na_v1.5$ channels into the BLMs with their extracellular sides facing the *trans* side. The probability of observing either single- or multichannel activities was 67% (Fig. 3) under conditions in which vesicle fusion was performed under centrifugation at 800–900 rpm (35–44 $\times$ *g*) for 5–10 min. Although the observed $Na_v1.5$ single-channel traces showed no significant signs of inactivation during the recording period, the possibility that the inactivation of macroscopic currents might have been hidden in the large saturating transient current during the first ~90 ms after the voltage step cannot be excluded. Possible macroscopic events, however, could not be resolved due to the large transient current, which probably resulted from a clamp delay caused by charging across the BLMs with a high capacitance (usually 50–100 pF). Similar slow transients after the voltage steps have also been reported for voltage-gated potassium channels reconstituted in BLM systems (37,42).

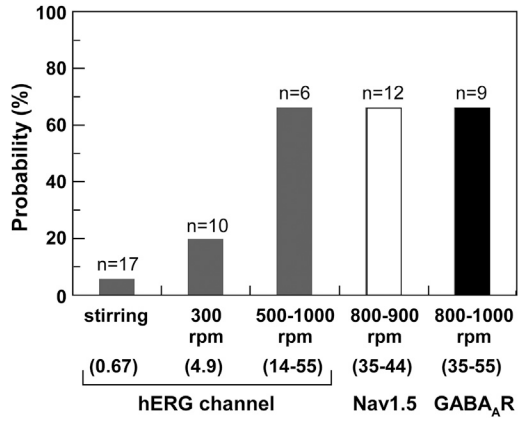

FIGURE 3 Percentage of recording single- or multichannel currents for hERG, $Na_v1.5$, and $GABA_AR$ channels under various conditions of channel incorporation. Numbers in parentheses indicate the relative centrifugal force ($\times g$). The rotation radius for the centrifugation was 49 mm. The relative centrifugal force in the case of stirring was calculated using a rotation radius of 6 mm and a rotation number of 100 rpm. The size of the microaperture was 45–55 μm for the hERG channel, 18–40 μm for the $Na_v1.5$ channel, and 25–40 μm for the $GABA_AR$ channel, respectively.

To demonstrate that channel reconstitution based on centrifugation is generally applicable to various ion channel proteins, we examined the centrifugal incorporation of human $GABA_AR$, a ligand-gated anion channel that mediates inhibitory neurotransmission in the central nervous system (43). $GABA_AR$ has been identified not only as a major target for designing anti-anxiety and anesthetic drugs (2,44) but also as a recommended target for assessing potential side effects of drugs (4). Fig. 5 *a* shows examples of single-channel recordings from BLMs after centrifugation with membrane vesicles containing $\alpha1\beta2\gamma2$-type $GABA_AR$ at 800 rpm. Stepwise currents were clearly observed with a single-channel conductance of 25 pS, which was close to a previously reported value (25–27 pS) for $\alpha1\beta2\gamma2$ $GABA_AR$ expressed in HEK 293 cells (45,46). The channel activities were only observed in the presence of GABA (*trans* side) and were completely blocked by the addition of picrotoxin (*trans* side), a specific blocker for $GABA_AR$ (Fig. 5 *b*). These channel properties confirmed the functional incorporation of $GABA_AR$ into the BLMs. The probability of observing either single- or multichannel activities was 67% (Fig. 3) under conditions in which vesicle fusion was performed

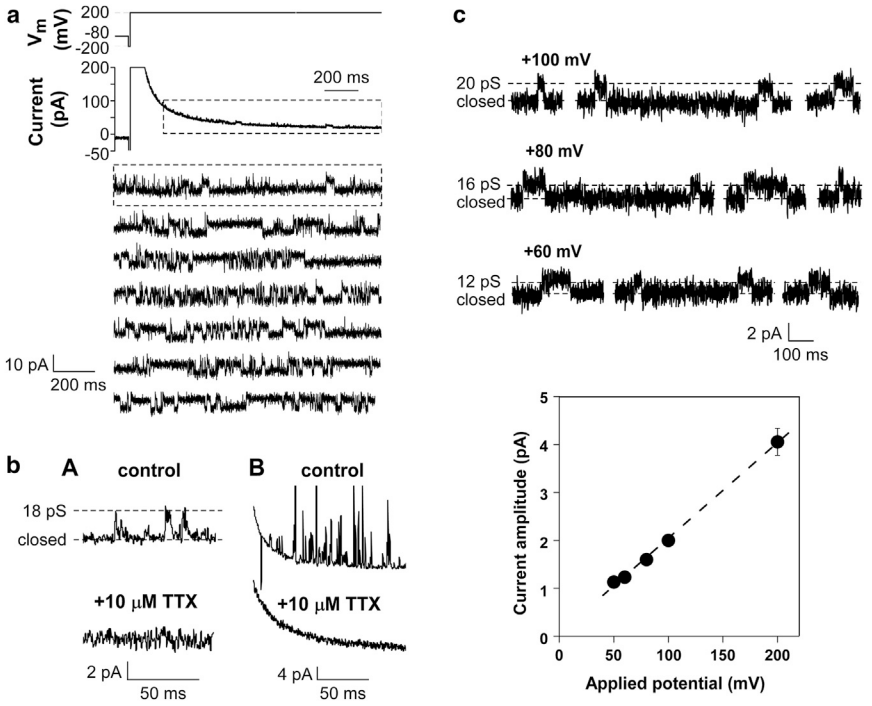

FIGURE 4 Examples of $Na_v1.5$ channel currents recorded after centrifugation at 800–900 rpm. (*a*) Typical $Na_v1.5$ single-channel currents obtained using a voltage protocol with a 10 ms step to −200 mV, followed by an 1800 ms step to +200 mV. The large and slow transient current observed in the raw current (*top trace*) was fitted to the equation $y = y_0 + A_1 \exp\{-(t - t_0)/\tau_1\} + A_2 \exp\{-(t - t_0)/\tau_2\}$, where t is a variable, y is a function of t, t_0 is a constant (0.19 s), and y_0, A_1, A_2, t_0, τ_1, and τ_2 are fitting parameters. Since the current at short times after the voltage step to +200 mV was saturated at 200 pA, $(t - t_0)$ was fitted so that the fitting started around the point where the current became smaller than 200 pA. This point (t = 0.19 s) corresponds to ~90 ms after the step to + 200 mV. The fitted current was subtracted from the raw current, yielding the current trace shown in the second trace. Seven representative currents obtained in the same manner from the same membrane are shown. The current was recorded after centrifugation at 800 rpm for 5 min. (*b*) Inhibition of $Na_v1.5$ channel activities by TTX at the single-channel level (*A*) and the multichannel level (*B*). The currents were recorded after centrifugation at 900 rpm for 5 min. The same voltage protocol shown in (*a*) was used. TTX was added to the *trans* solution to produce a concentration of 10 μM. (*c*) Single $Na_v1.5$ channel currents recorded at an applied potential of +100, +80 and +60 mV after a 10-ms pulse to -200 mV (*top*). Single-channel current-voltage relationship for $Na_v1.5$ (*bottom*). The error bar indicates the SEM (n=5). The current was recorded after centrifugation at 800 rpm for 5 min.

via centrifugation at 800–1000 rpm (35–55 × *g*) for 5–15 min. Therefore, efficient channel incorporation into BLMs was also achieved for $GABA_AR$ via vesicle fusion under centrifugation.

In total, an incorporation probability of 67% (18 out of 27 BLMs) was obtained for the hERG, $Na_v1.5$, and $GABA_AR$ channels when they were prepared under optimal centrifugal conditions (500–1000 rpm (14–55 × *g*) for hERG from CHO cells, 800–900 rpm (35–44 × *g*) for $Na_v1.5$ from HEK 293 cells, and 800–1000 rpm (35–55 × *g*) for $GABA_AR$ from HEK 293 cells). These results demonstrate that centrifugation is useful for accelerating channel integration into BLMs. The optimum centrifugal range appeared to be dependent on the type of channel and cells expressing the channels, which probably reflects the difference in the lipid compositions for respective membrane vesicles (Supporting Materials and Methods). However, centrifugation at 800–900 rpm (35–44 × *g*) generally resulted in efficient incorporation (73%, 11 out of 15 BLMs). At 1000 rpm (55 × *g*) the incorporation probability decreased to 45% (5 out of 11 BLMs), probably due to the increased percentage (36%) of broken BLMs that were produced under a higher centrifugal force. The probability of BLM rupture was higher in the presence of membrane vesicles: 83% of BLMs (10 out of 12 BLMs) survived centrifugation at 1000 rpm in the absence of membrane vesicles. Owing to the tapered aperture edges (Fig. S2), the BLMs that formed in the microapertures in the Si chips were sufficiently stable to tolerate centrifugal forces up to 1000 rpm (55 × *g*).

Fusion force versus centrifugal force

Membrane fusion has attracted attention both as a critical step in creating a BLM reconstitution system and as an essential step in biological exocytosis. AFM measurements of the fusion force between two lipid bilayers floated on BLMs supported on glass surfaces indicate that applied forces in the range of ~100–500 pN are needed to induce fusion of two contacting lipid bilayers (47). When SNARE proteins, which mediate fusion in eukaryotic cell membranes, were present in the two lipid bilayers, the required force decreased to 50–200 pN (48). To compare the magnitude of the centrifugal force utilized here with the reported fusion force, we estimated the size and density of membrane vesicles to calculate the centrifugal force ($m\ (\rho - \sigma)\ r\omega^2$, where m is the mass of the membrane vesicle; ρ and σ are the densities of the membrane vesicle and recording solution, respectively; r is the radius of the centrifuge; and ω is the angular velocity). The distribution of vesicle diameter varied among the different samples of membrane vesicles and the diameter at the peak of the distribution histogram ranged from 200 to 400 nm (Fig. S3). The densities of the recording solution (σ) and membrane vesicle (ρ) were experimentally estimated to be 1 g/cm^3 and 2 g/cm^3,

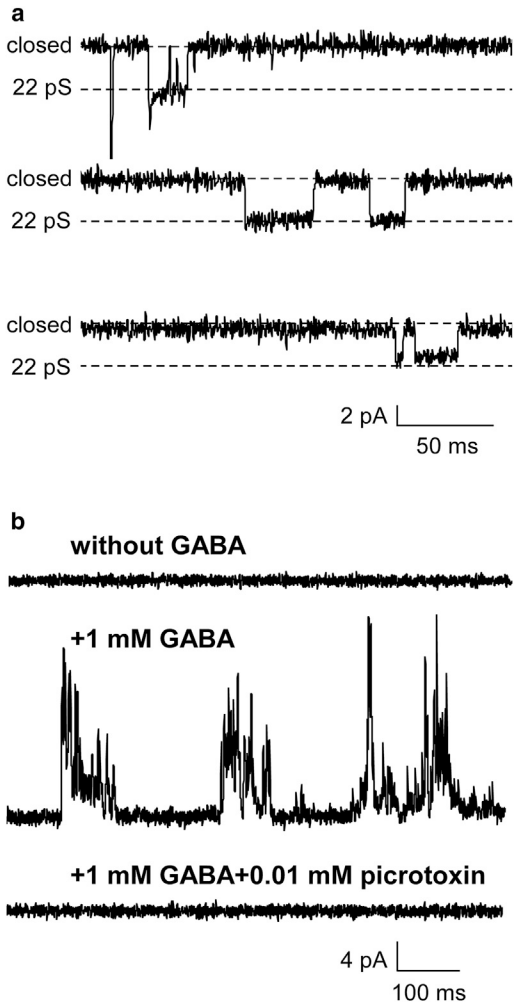

FIGURE 5 Examples of $GABA_AR$ channel currents recorded after centrifugation at 800–1000 rpm. (*a*) Typical single-channel currents at an applied potential of −200 mV. GABA was added to the *trans* solution to produce a concentration of 1 mM. The current was recorded after centrifugation at 800 rpm for 10 min and 1000 rpm for 5 min. (*b*) Typical $GABA_AR$ multichannel currents at an applied potential of +100 mV. GABA and picrotoxin were added to the *trans* solution to give a concentration of 1 mM and 0.01 mM, respectively. The current was recorded after centrifugation at 900 rpm for 10 min.

respectively (Supporting Materials and Methods). The centrifugal force for membrane vesicles with a diameter of 200–400 nm when the vesicles were spun at 1000 rpm with a rotation radius (r) of 49 mm was calculated to be $2.2 \times 10^{-3} - 1.7 \times 10^{-2}$ pN. The calculated centrifugal force was ~4–5 orders of magnitude smaller than that required for fusion between two lipid bilayers in contact with one another (~100–500 pN). This small centrifugal force was still sufficient to deliver the membrane vesicles to the surface of the BLMs (Fig. 2). These results strongly suggest that a centrifugal enhancement in vesicle fusion was attained, not by accelerating the fusion process but by accelerating the delivery of membrane vesicles to dock at the BLMs. It was previously reported that docking is a rate-limiting step in vesicle-vesicle fusion (49) and that a slow fusion rate could arise from insufficient docking (50). Our approach also focused on the docking state. The centrifugal force increased the number of membrane vesicles docking at BLMs, leading to an enhanced incorporation of human ion channels into the BLMs.

CONCLUSIONS

Here, we have reported on the efficient incorporation of human ion channels into solvent-free BLMs by using centrifugal force to deliver membrane vesicles to the surface of the BLMs. Centrifugal force, which is commonly used for the purification of a variety of proteins, including ion channels, is highly compatible with ion channel proteins, and no significant effect on channel activities by centrifugation is expected. The centrifugation of BLMs with membrane vesicles containing human ion channels (hERG, human $Na_v1.5$, and human $GABA_AR$) resulted in efficient vesicle fusion, and ion channel currents were recorded from 67% of the BLMs examined. All of the hERG, $Na_v1.5$, and $GABA_AR$ channels exhibited their respective characteristic properties, confirming that these channels were intact after centrifugal incorporation was achieved. Owing to the robustness of the BLMs that formed in tapered apertures, the centrifugal force served to accelerate channel incorporation into solvent-free BLMs, which are expected to have fewer potential fusion sites compared with solvent-containing BLMs. The incorporation probability could be further enhanced by combining the approach presented here with other methods that accelerate the fusion steps, such as those that employ osmotic salt gradients and nystatin-ergosterol. The difficulty of integrating ion channels into BLMs has been a major bottleneck to the construction of membrane platforms for the functional analysis of ion channels. The methodology reported here for the efficient incorporation of channels into solvent-free BLMs has the potential to serve as a new high-throughput platform for recording human channel activities that would be an alternative to the patch-clamp method.

SUPPORTING MATERIAL

Supporting Materials and Methods and three figures are available at http://www.biophysj.org/biophysj/supplemental/S0006-3495(16)30173-4.

AUTHOR CONTRIBUTIONS

A.H.-I. conceived the study, designed the experiments, and wrote the manuscript with contributions from D.T., H.Y., Y.K., and M.N. Y.I., M.Y., S.A., D.T., R.M., and K.I. performed the experiments. All authors discussed the results and commented on the manuscript.

ACKNOWLEDGMENTS

This work was supported by Grants-in-Aid for Scientific Research from the Japan Society for the Promotion of Science (15H03822 and 26620111) and

the CREST program of the Japan Science and Technology Agency. Financial support was also provided by the Asahi Glass Foundation and Nakatani Foundation.

SUPPORTING CITATIONS

References (51,52) appear in the Supporting Material.

REFERENCES

1. Rask-Andersen, M., M. S. Almén, and H. B. Schiöth. 2011. Trends in the exploitation of novel drug targets. *Nat. Rev. Drug Discov.* 10:579–590.
2. Clare, J. J. 2010. Targeting ion channels for drug discovery. *Discov. Med.* 9:253–260.
3. Dunlop, J., M. Bowlby, …, R. Arias. 2008. High-throughput electrophysiology: an emerging paradigm for ion-channel screening and physiology. *Nat. Rev. Drug Discov.* 7:358–368.
4. Bowes, J., A. J. Brown, …, S. Whitebread. 2012. Reducing safety-related drug attrition: the use of *in vitro* pharmacological profiling. *Nat. Rev. Drug Discov.* 11:909–922.
5. Hirano-Iwata, A., Y. Ishinari, …, M. Niwano. 2015. Micro- and nanotechnologies for lipid bilayer-based ion-channel functional assays. *Chem. Asian J.* 10:1266–1274.
6. Kongsuphol, P., K. B. Fang, and Z. Ding. 2013. Lipid bilayer technologies in ion channel recordings and their potential in drug screening assay. *Sens. Actuators B Chem.* 185:530–542.
7. Han, X., A. Studer, …, L. X. Tiefenauer. 2007. Nanopore arrays for stable and functional free-standing lipid bilayers. *Adv. Mater.* 19:4466–4470.
8. Ervin, E. N., R. J. White, and H. S. White. 2009. Sensitivity and signal complexity as a function of the number of ion channels in a stochastic sensor. *Anal. Chem.* 81:533–537.
9. Kawano, R., T. Osaki, …, S. Takeuchi. 2010. A polymer-based nanopore-integrated microfluidic device for generating stable bilayer lipid membranes. *Small.* 6:2100–2104.
10. Römer, W., and C. Steinem. 2004. Impedance analysis and single-channel recordings on nano-black lipid membranes based on porous alumina. *Biophys. J.* 86:955–965.
11. Hirano-Iwata, A., K. Aoto, …, M. Niwano. 2010. Free-standing lipid bilayers in silicon chips-membrane stabilization based on microfabricated apertures with a nanometer-scale smoothness. *Langmuir.* 26:1949–1952.
12. Oshima, A., A. Hirano-Iwata, …, M. Niwano. 2013. Reconstitution of human *ether-a-go-go*-related gene channels in microfabricated silicon chips. *Anal. Chem.* 85:4363–4369.
13. Eray, M., N. S. Dogan, …, B. J. Van Wie. 1994. Highly stable bilayer lipid membranes (BLMs) formed on microfabricated polyimide apertures. *Biosens. Bioelectron.* 9:343–351.
14. Kalsi, S., A. M. Powl, …, M. R. R. de Planque. 2014. Shaped apertures in photoresist films enhance the lifetime and mechanical stability of suspended lipid bilayers. *Biophys. J.* 106:1650–1659.
15. Hirano-Iwata, A., M. Niwano, and M. Sugawara. 2008. The design of molecular sensing interfaces with lipid-bilayer assemblies. *Trends Analyt. Chem.* 27:512–520.
16. Demarche, S., K. Sugihara, …, J. Vörös. 2011. Techniques for recording reconstituted ion channels. *Analyst.* 136:1077–1089.
17. Kasai, H., N. Takahashi, and H. Tokumaru. 2012. Distinct initial SNARE configurations underlying the diversity of exocytosis. *Physiol. Rev.* 92:1915–1964.
18. Cohen, F. S., J. Zimmerberg, and A. Finkelstein. 1980. Fusion of phospholipid vesicles with planar phospholipid bilayer membranes. II. Incorporation of a vesicular membrane marker into the planar membrane. *J. Gen. Physiol.* 75:251–270.
19. Ide, T., T. Kobayashi, and M. Hirano. 2008. Lipid bilayers at the gel interface for single ion channel recordings. *Anal. Chem.* 80:7792–7795.
20. Woodbury, D. J., and C. Miller. 1990. Nystatin-induced liposome fusion. A versatile approach to ion channel reconstitution into planar bilayers. *Biophys. J.* 58:833–839.
21. Zagnoni, M., M. E. Sandison, …, H. Morgan. 2007. Controlled delivery of proteins into bilayer lipid membranes on chip. *Lab Chip.* 7:1176–1183.
22. Studer, A., S. Demarche, …, L. Tiefenauer. 2011. Integration and recording of a reconstituted voltage-gated sodium channel in planar lipid bilayers. *Biosens. Bioelectron.* 26:1924–1928.
23. Nelson, N., R. Anholt, …, M. Montal. 1980. Reconstitution of purified acetylcholine receptors with functional ion channels in planar lipid bilayers. *Proc. Natl. Acad. Sci. USA.* 77:3057–3061.
24. Leptihn, S., J. R. Thompson, …, M. I. Wallace. 2011. In vitro reconstitution of eukaryotic ion channels using droplet interface bilayers. *J. Am. Chem. Soc.* 133:9370–9375.
25. El-Arabi, A. M., C. S. Salazar, and J. J. Schmidt. 2012. Ion channel drug potency assay with an artificial bilayer chip. *Lab Chip.* 12:2409–2413.
26. Maurer, J. A., V. E. White, …, J. L. Nadeau. 2007. Reconstitution of ion channels in agarose-supported silicon orifices. *Biosens. Bioelectron.* 22:2577–2584.
27. Kawano, R., Y. Tsuji, …, S. Takeuchi. 2013. Automated parallel recordings of topologically identified single ion channels. *Sci. Rep.* 3:1995.
28. Cohen, F. S., M. H. Akabas, …, A. Finkelstein. 1984. Parameters affecting the fusion of unilamellar phospholipid vesicles with planar bilayer membranes. *J. Cell Biol.* 98:1054–1062.
29. Gutsmann, T., T. Heimburg, …, M. Winterhalter. 2015. Protein reconstitution into freestanding planar lipid membranes for electrophysiological characterization. *Nat. Protoc.* 10:188–198.
30. Perin, M. S., and R. C. MacDonald. 1989. Interactions of liposomes with planar bilayer membranes. *J. Membr. Biol.* 109:221–232.
31. Oshima, A., A. Hirano-Iwata, …, M. Niwano. 2012. Mechanically stable lipid bilayers in Teflon-coated silicon chips for single-channel recordings. *Micro Nanosyst.* 4:2–7.
32. Zou, A., M. E. Curran, …, M. C. Sanguinetti. 1997. Single HERG delayed rectifier K^+ channels expressed in *Xenopus* oocytes. *Am. J. Physiol.* 272:H1309–H1314.
33. Chanturiya, A., L. V. Chernomordik, and J. Zimmerberg. 1997. Flickering fusion pores comparable with initial exocytotic pores occur in protein-free phospholipid bilayers. *Proc. Natl. Acad. Sci. USA.* 94:14423–14428.
34. Chernomordik, L. V., and M. M. Kozlov. 2008. Mechanics of membrane fusion. *Nat. Struct. Mol. Biol.* 15:675–683.
35. Sanguinetti, M. C., and M. Tristani-Firouzi. 2006. hERG potassium channels and cardiac arrhythmia. *Nature.* 440:463–469.
36. Vandenberg, J. I., M. D. Perry, …, A. P. Hill. 2012. hERG K^+ channels: structure, function, and clinical significance. *Physiol. Rev.* 92:1393–1478.
37. Vijayvergiya, V., S. Acharya, …, J. Schmidt. 2015. Single channel and ensemble hERG conductance measured in droplet bilayers. *Biomed. Microdevices.* 17:12.
38. Amin, A. S., A. Asghari-Roodsari, and H. L. Tan. 2010. Cardiac sodium channelopathies. *Pflugers Arch.* 460:223–237.
39. Beyder, A., J. L. Rae, …, G. Farrugia. 2010. Mechanosensitivity of $Na_v1.5$, a voltage-sensitive sodium channel. *J. Physiol.* 588:4969–4985.
40. McNulty, M. M., G. B. Edgerton, …, G. M. Lipkind. 2007. Charge at the lidocaine binding site residue Phe-1759 affects permeation in human cardiac voltage-gated sodium channels. *J. Physiol.* 581:741–755.
41. Klein, G., A. Gardiwal, …, D. Breitmeier. 2007. Effect of ethanol on cardiac single sodium channel gating. *Forensic Sci. Int.* 171:131–135.

42. Hutter, I., E. Müller, …, L. Tiefenauer. 2013. Polymer-based microfluidic device for measuring membrane protein activities. *Microfluid Nanofluid.* 14:421–429.

43. Karim, N., P. Wellendorph, …, M. Chebib. 2013. Potency of GABA at human recombinant $GABA_A$ receptors expressed in *Xenopus* oocytes: a mini review. *Amino Acids.* 44:1139–1149.

44. Mathie, A. 2010. Ion channels as novel therapeutic targets in the treatment of pain. *J. Pharm. Pharmacol.* 62:1089–1095.

45. Dixon, C., P. Sah, …, A. Keramidas. 2014. $GABA_A$ receptor α and γ subunits shape synaptic currents via different mechanisms. *J. Biol. Chem.* 289:5399–5411.

46. Keramidas, A., and N. L. Harrison. 2008. Agonist-dependent single channel current and gating in $\alpha_4\beta_2\delta$ and $\alpha_1\beta_2\gamma_{2S}$ $GABA_A$ receptors. *J. Gen. Physiol.* 131:163–181.

47. Abdulreda, M. H., and V. T. Moy. 2007. Atomic force microscope studies of the fusion of floating lipid bilayers. *Biophys. J.* 92:4369–4378.

48. Abdulreda, M. H., A. Bhalla, …, V. T. Moy. 2008. Atomic force microscope spectroscopy reveals a hemifusion intermediate during soluble *N*-ethylmaleimide-sensitive factor-attachment protein receptors-mediated membrane fusion. *Biophys. J.* 94:648–655.

49. Smith, E. A., and J. C. Weisshaar. 2011. Docking, not fusion, as the rate-limiting step in a SNARE-driven vesicle fusion assay. *Biophys. J.* 100:2141–2150.

50. Liu, T., W. C. Tucker, …, J. C. Weisshaar. 2005. SNARE-driven, 25-millisecond vesicle fusion in vitro. *Biophys. J.* 89:2458–2472.

51. Vogel, R., G. Willmott, …, M. Trau. 2011. Quantitative sizing of nano/microparticles with a tunable elastomeric pore sensor. *Anal. Chem.* 83:3499–3506.

52. Colby, A. H., Y. L. Colson, and M. W. Grinstaff. 2013. Microscopy and tunable resistive pulse sensing characterization of the swelling of pH-responsive, polymeric expansile nanoparticles. *Nanoscale.* 5:3496–3504.

Biophysical Journal, Volume *110*

Supplemental Information

Reconstitution of Human Ion Channels into Solvent-free Lipid Bilayers Enhanced by Centrifugal Forces

Ayumi Hirano-Iwata, Yutaka Ishinari, Miyu Yoshida, Shun Araki, Daisuke Tadaki, Ryusuke Miyata, Kenichi Ishibashi, Hideaki Yamamoto, Yasuo Kimura, and Michio Niwano

Biophysical Journal

Supporting Material

Reconstitution of Human Ion Channels into Solvent-free Lipid Bilayers Enhanced by Centrifugal Forces

Ayumi Hirano-Iwata,[1,*] Yutaka Ishinari,[1] Miyu Yoshida,[1] Shun Araki,[1] Daisuke Tadaki,[1] Ryusuke Miyata,[1] Kenichi Ishibashi,[2] Hideaki Yamamoto,[3] Yasuo Kimura,[4] and Michio Niwano[1,5]

[1]Graduate School of Biomedical Engineering, Tohoku University, Aoba, Sendai, Japan; [2]Hang-Ichi Corporation, Naka, Yokohama, Japan; [3]Frontier Research Institute for Interdisciplinary Sciences, Tohoku University, Aoba, Sendai, Japan; [4]Department of Electric and Electronic Engineering, School of Engineering, Tokyo University of Technology, Hachioji, Tokyo, Japan; and [5]Laboratory for Nanoelectronics and Spintronics, Research Institute of Electrical Communication, Tohoku University, Aoba, Sendai, Japan

*Correspondence: ahirano@bme.tohoku.ac.jp

MATERIALS AND METHODS

Fabrication of microapertures.

Microapertures were fabricated in silicon (Si) chips, according to the procedures described in ref. 1 (Fig. S1). In brief, a FZ Si (100) wafer, one side of which was coated with a Si_3N_4 layer, was thermally oxidized in dry oxygen, and then the Si_3N_4 side was coated with SiO_2 by RF sputtering method. The thermal oxide layer was photolithographically patterned, and anisotropically etched in tetramethylammonium hydroxide. Then SiO_2 was sputtered onto the Si side to cover bare Si_3N_4 and Si surfaces formed during the anisotropic etching. After photolithographic patterning, circular holes were formed in the Si_3N_4 layer by isotropic etching in 85% phosphoric acid at 150 ˚C. The SiO_2 layer beneath the holes was then removed by 5% hydrofluoric acid to form apertures. Next a SiO_2 layer was grown on the surface of the Si chips containing apertures by wet thermal oxidation for 1 h. A layer of SU8–3010 photoresist (MicroChem, Newton, MA) was spun onto a dummy wafer, and the chip was placed on the SU8-3010 layer from the Si_3N_4 side. A Teflon-AF1601 solution (DuPont Fluoroproducts, Wilmington, DE) was then spun onto the chip and the solvent (FC-40) was allowed to evaporate at 95 ˚C. Teflon-AF around the apertures was lifted off by soaking in hot Remover 1165. Finally, the chips were washed thoroughly with isopropanol, ethanol, acetonitrile, acetone and chloroform.

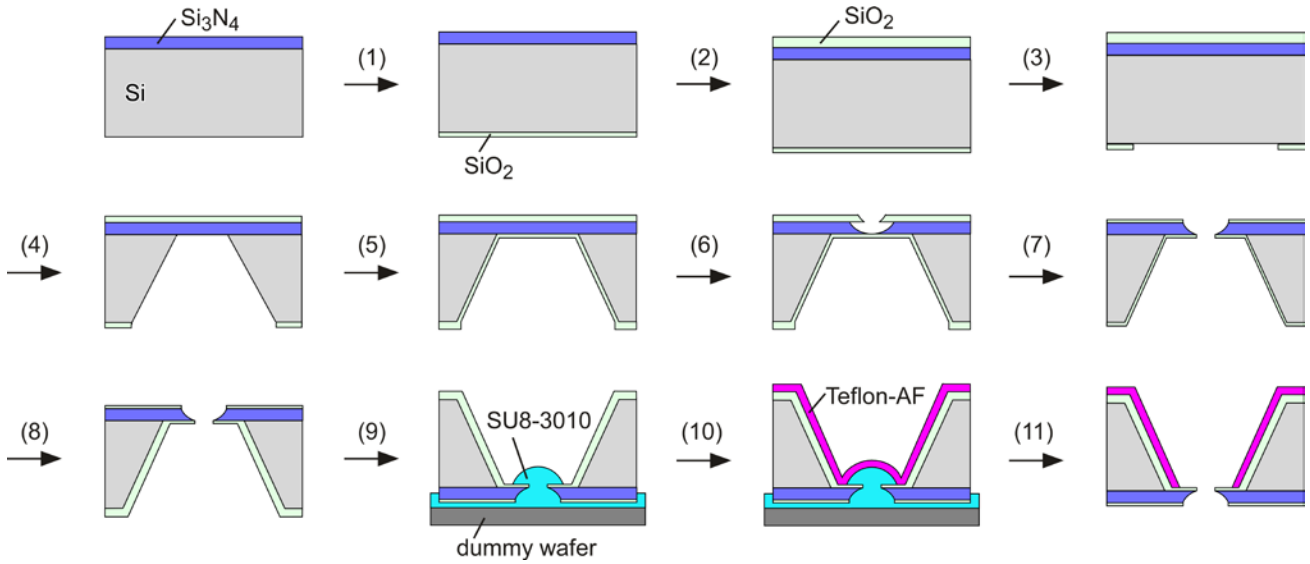

Fig. S1. Procedures for fabricating microapertures: (1) Thermal oxidation; (2) sputtering of SiO_2; (3) patterning of the thermal oxide layer; (4) anisotropic etching of Si; (5) RF sputtering of SiO_2; (6) patterning and isotropic etching of Si_3N_4; (7) SiO_2 removal; (8) wet thermal oxidation; (9) placing the Si chip on an SU8-3010 layer; (10) spin coating of Teflon-AF; (11) lifting off the Teflon-AF layer around the aperture.

Analysis of size distribution and density of membrane vesicles.

Size distribution of membrane vesicles was obtained using qNano (Izon Science, Oxford, United Kingdom) according to standard operating procedures (2, 3). Briefly, a nanopore membrane (NP800) was mounted onto the stretching pins of the qNano and stretched to a pin-to-pin width of 45 mm - 47 mm. Recording solution (120 mM KCl, 10 mM HEPES, pH 7.2 with KOH) was added to the both cell chambers which contained an Ag/AgCl electrode each, below and above the nanopore membrane. After removing air bubbles trapped in the nanopore, a voltage is applied across the membrane to establish a baseline electrical current through the nanopore. The solution in the upper cell chamber was then replaced with a solution containing standard particles of known size or membrane vesicles. Vesicles (particles) translocating the nanopore was detected as transient current blockade. The size and concentration of vesicles (particles) was obtained based on their relationship to the magnitude of

individual blockade currents and the rate of the blockade events, respectively. The density of membrane vesicle (ρ) was estimated based on the following equation,

$$\rho \sum_{d}^{d_{\max}} V_d C_d + \sigma \left(1 - \sum_{d}^{d_{\max}} V_d C_d \right) = \omega$$

where ρ and ω are density (g/mL) of the recording solution and sample solution containing membrane vesicles, respectively, and V_d and C_d are volume and concentration (particles/mL) of vesicles with a diameter of *d*, respectively.

Analysis of lipid compositions in cell membranes by using thin-layer chromatography (TLC) .

Lipid compositions in cell membranes of Chinese hamster ovary (CHO) cell lines expressing the hERG channels, Human Embryonic Kidney (HEK) 293 cell lines expressing the human $Na_v1.5$ and human $\alpha1\beta2\gamma2$ $GABA_A$ receptor channels were analyzed with TLC. In brief, the cell lines stored in liquid nitrogen were thawed and sonicated in phosphate buffered saline. Then the cell samples were mixed well with chloroform and methanol. After addition of water and chloroform, chloroform layer was collected and concentrated with nitrogen stream. TLC analysis was made using HPTLC plates of silica gel 60 (Merck Millipore, Darmstadt, Germany) and a software JustTLC (Sweday, Sweden). The weight % of each lipid component, i.e., phosphatidylcholine (PC), phosphatidylethanolamine (PE) and cholesterol (Chol), thus analyzed was as follows: PC 43%, PE 25% and Chol 32% for CHO cells expressing the hERG channels, PC 40%, PE 35% and Chol 25% for HEK 293 cells expressing the $GABA_A$ receptor channels, and PC 49%, PE 26% and Chol 25% for HEK 293 cells expressing the $Na_v1.5$ receptor channels. Interestingly, cells containing higher amounts of PE and Chol compared with PC appeared to be robust against centrifugal forces and showed wider optimum centrifugal ranges for the channel integration into bilayer lipid membranes (BLMs).

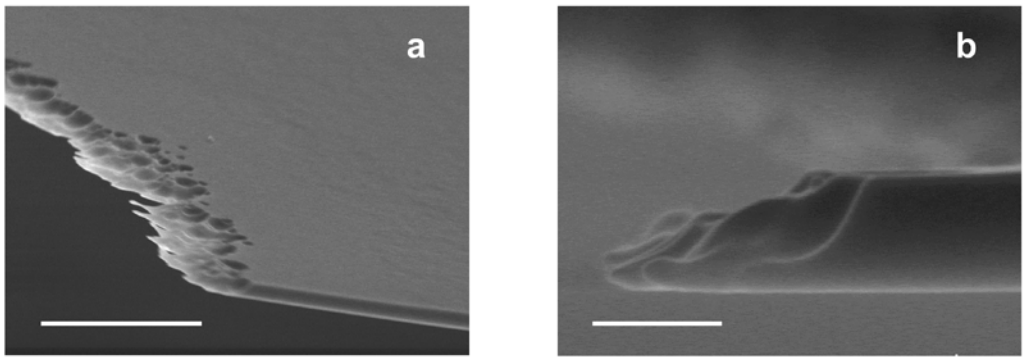

Fig. S2. Scanning electron microscopy (SEM) images of an aperture edge. (a) Overhead view. Scale bar 2 μm, tilt 66.8°. (b) Cross-sectional view. Scale bar 300 nm.

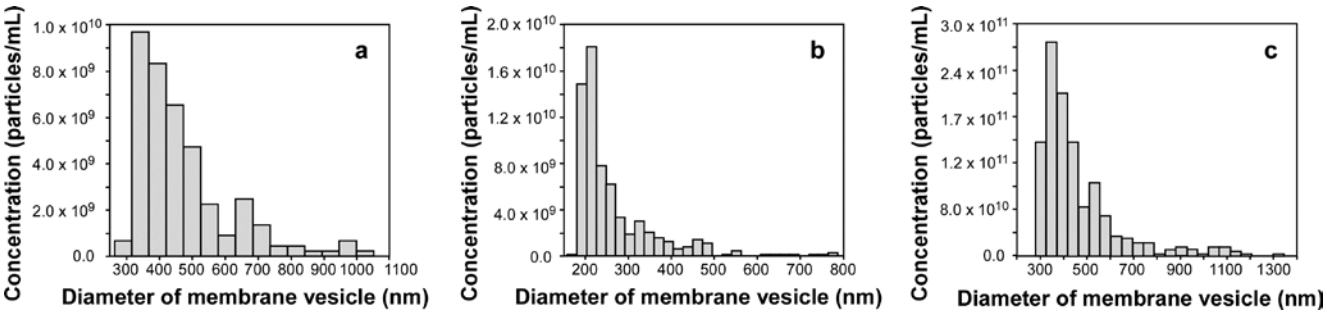

Fig. S3. Size distribution of membrane vesicles. Samples a-c were vesicles extracted from different cultures of CHO cell lines expressing hERG channels. Each sample was diluted 10-100 times with recording solution (120 mM KCl, 10 mM HEPES, pH 7.2 with KOH) and size distribution was determined using qNANO.

Supporting References

(1) Oshima, A., A. Hirano-Iwata, …, M. Niwano. 2012. Mechanically stable lipid bilayers in Teflon-coated silicon chips for single-channel recordings. *Micro & Nanosystems*. 4:2-7.

(2) Vogel, R., G. Willmott, …, M. Trau. 2011. Quantitative sizing of nano/microparticles with a tunable elastomeric pore sensor. *Anal. Chem*. 83: 3499-3506.

(3) Colby, A. H., Y. L. Colson, and M. W. Grinstaff. 2013. Microscopy and tunable resistive pulse sensing characterization of the swelling of pH-responsive, polymeric expansile nanoparticles. *Nanoscale*. 5:3496-3504.